nature biotechnology

Supplementary information

https://doi.org/10.1038/s41587-024-02535-2

Multiplexed inhibition of immunosuppressive genes with Cas13d for combinatorial cancer immunotherapy

In the format provided by the authors and unedited

Supplementary Information

Content

Figure S1

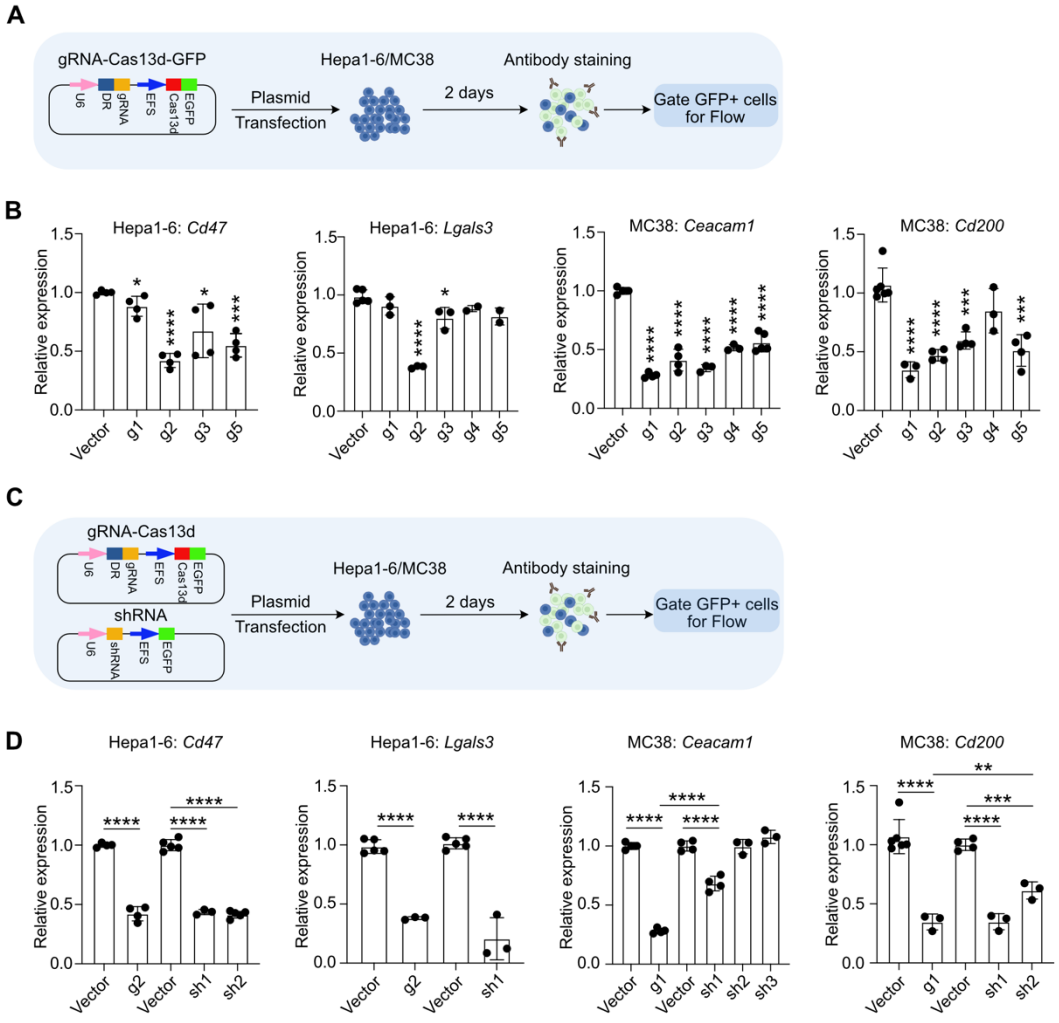

Figure S1. Cas13d-mediated silencing of endogenous immunosuppressive genes in cancer cells

A. Schematic of the experimental approach to identify efficient Cas13d-gRNAs targeting of various immunosuppressive genes. An all-in-one plasmid including gRNA, Cas13 and EGFP was transfected into Hepa1-6 or MC38 cells. Two days after plasmid transfection, target gene expression was analyzed by flow cytometry analysis. Successfully transfected cells were gated by GFP^+ cells.

B. Knockdown efficiency of gRNAs targeting different immunosuppressive genes in various cancer cell lines. *Cd47* (n=4) and *Lgals3 (Galectin3,* n>=2*)* were tested in Hepa1-6 cells, and *Ceacam1(Cd66a,* n>=3*)* and *Cd200* (n>=3) were tested in MC38 cells. Data are expressed as the relative mean of fluorescent intensity (MFI). The gene expression level of vector group was normalized to 1.

C. Schematic of the experimental approach to compare knockdown efficiency between Cas13d-gRNAs and shRNA. The Cas13d all-in-one (gRNA-Cas13-EGFP) or shRNA-EGFP plasmid was transfected into Hepa1-6 or MC38 cells. Two days after transfection, target gene expression was tested by flow cytometry analysis. Successfully transfected cells were gated by GFP^+ cells.

D. Comparison of the Cas13d-gRNA-mediated and shRNA-mediated target knockdown. *Cd47* and *Lgals3 (Galectin3)* were tested in Hepa1-6 cells, and *Ceacam1(Cd66a)* and *Cd200* were tested in MC38 cells. Data are expressed as the relative mean of fluorescent intensity (MFI). The gene expression level of vector group was normalized to 1. (n>=3, each group)

Data points in this figure are presented as mean ± s.e.m. Statistical significance was assessed by unpaired *t* test. * $p < 0.05$, ** $p < 0.01$, *** $p < 0.001$, **** $p < 0.0001$. Non-significant comparisons are not shown. Details of statistics in **Source Data and statistics** excel file.

Figure S2

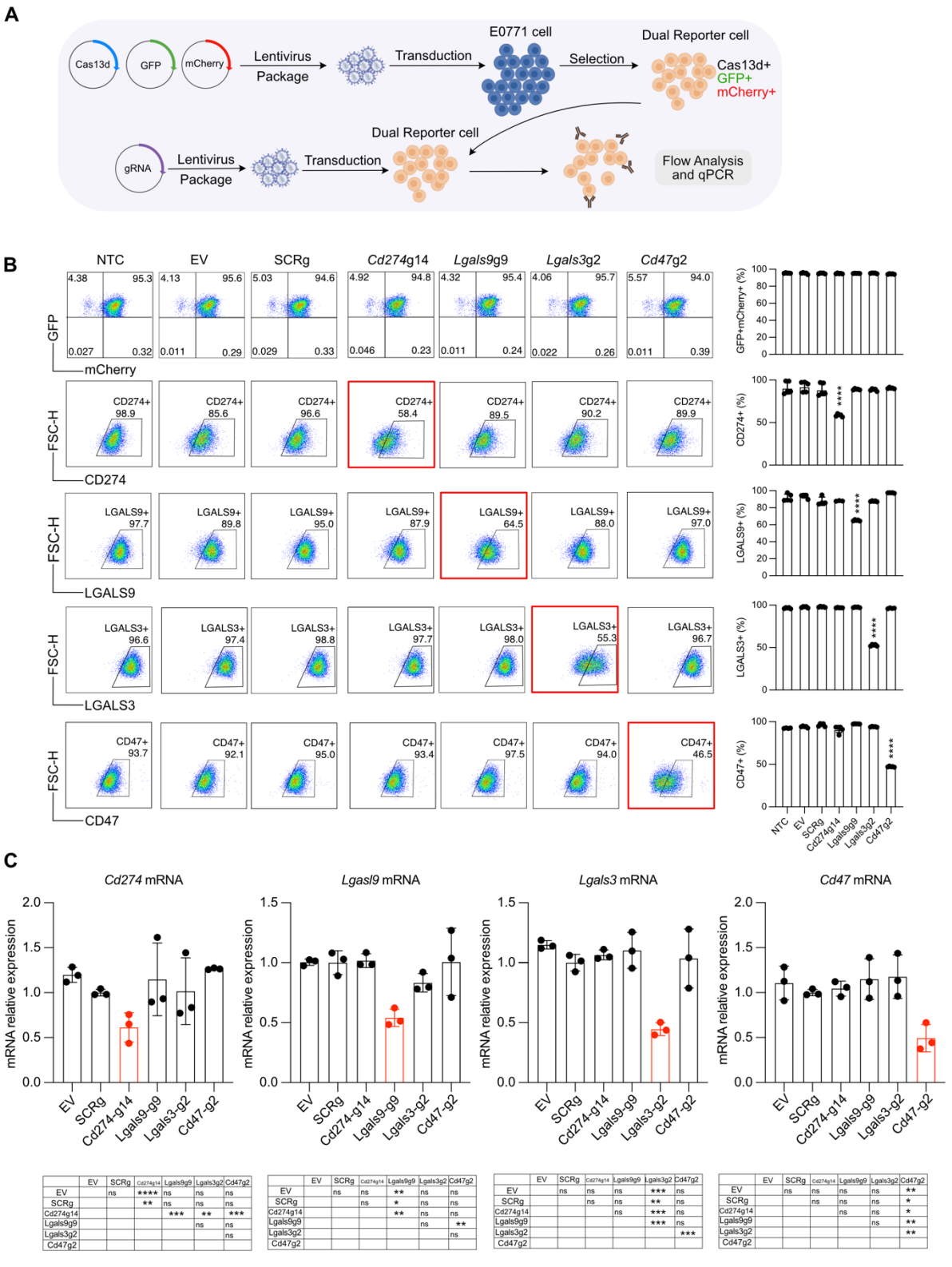

	EV	SCRg	Cd274g14	Lgals9g9	Lgals3g2	Cd47g2
EV		ns	****	ns	ns	ns
SCRg			**	ns	ns	ns
Cd274g14				***	**	***
Lgals9g9					ns	ns
Lgals3g2						ns
Cd47g2						

	EV	SCRg	Cd274g14	Lgals9g9	Lgals3g2	Cd47g2
EV		ns	ns	**	ns	ns
SCRg			ns	*	ns	ns
Cd274g14				**	ns	ns
Lgals9g9					ns	**
Lgals3g2						ns
Cd47g2						

	EV	SCRg	Cd274g14	Lgals9g9	Lgals3g2	Cd47g2
EV		ns	ns	ns	***	ns
SCRg			ns	ns	**	ns
Cd274g14				ns	***	ns
Lgals9g9					***	ns
Lgals3g2						***
Cd47g2						

	EV	SCRg	Cd274g14	Lgals9g9	Lgals3g2	Cd47g2
EV		ns	ns	ns	ns	**
SCRg			ns	ns	ns	*
Cd274g14				ns	ns	*
Lgals9g9					ns	**
Lgals3g2						**
Cd47g2						

Figure S2. Cas13d on-target and collateral activity when targeting endogenous immunosuppressive genes

A. Diagram of Cas13d collateral activity and analysis of on-target activity using a dual-GFP and mCherry reporter system. E0711 cell line was co-transduced with three lentiviruses (Cas13d-blasticidin, GFP and mCherry). The Cas13d-expressing dual reporter E0771 cells was selected with blasticidin and then sorted by GFP^+ $mCherry^+$ double positive cells. The dual reporter cells were then transduced with Cas13d-gRNA lentivirus. Then the GFP and mCherry fluorescent signal was determined by flow cytometry. The on-target gene expression was tested by flow cytometry and qPCR.
B. Flow cytometry analysis of E0771 dual-reporter cells after transduction with different gRNAs. NTC (Non-Transduced-Control), EV (Empty Vector), SCRg (scramble guide-RNA). (n>=3, each group)
C. RT-qPCR analysis of the target gene expression. The gene mRNA expression level of SCRg was normalized to 1. (n>=3, each group)
Data points in this figure are presented as mean ± s.e.m. Statistical significance was assessed by one-way ANOVA Tukey's multiple comparisons test, adjusted P Value (**B, C**). Multiple comparisons were summarized in the table below. * $p < 0.05$, ** $p < 0.01$, *** $p < 0.001$, **** $p < 0.0001$. Details of statistics in **Source Data and statistics** excel file.

Figure S3

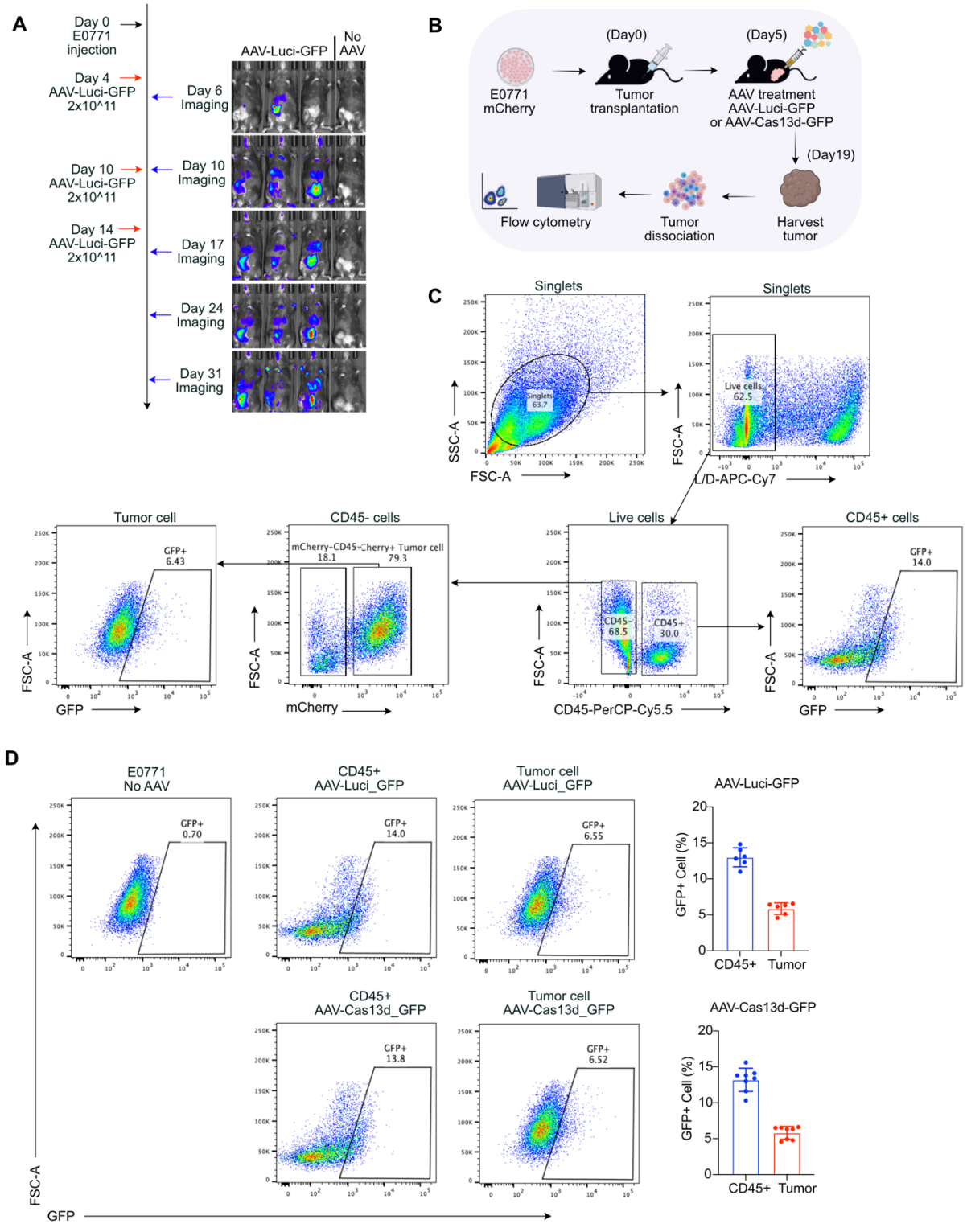

Figure S3. Persistent ectopic gene expression in tumors after intratumoral AAV injection

A. C57BL/6 mice were orthotopically injected with $2\times10^{\wedge6}$ E0771 cells. AAV-luciferase-GFP was then intratumorally injected at the indicated time points. *In-vivo* bioluminescence imaging was used to visualize luciferase activity.
B. Schematic of experimental design for analyzing AAV mediated gene expression in the TME. AAV-Luciferase-GFP and AAV-Cas13d-GFP were used, and GFP expression in TME cell populations were analyzed.
C. The gating strategy for flow cytometry staining panels are shown. Arrows indicate the parent population that the subsequent plot is gated on.
D. GFP^+ cells were gated to identify AAV-infected cells. E0771-mCherry cells without AAV infection were used to set the gating threshold for GFP. (n>=5, each group) Data points in this figure are presented as mean ± s.e.m. Details could be found in **Source Data and statistics** excel file.

Figure S4

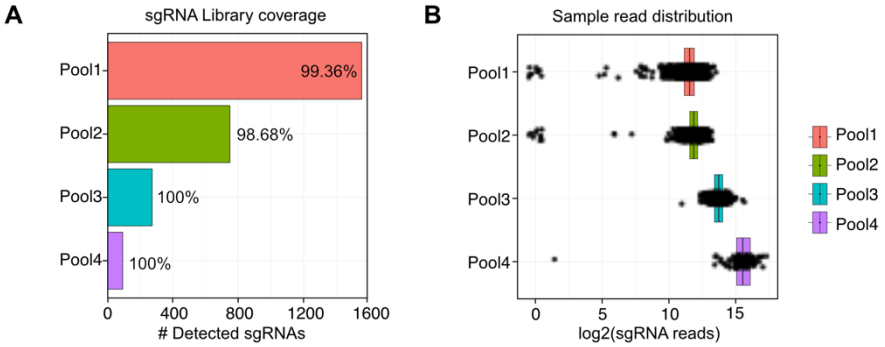

Figure S4. Library representation of four MUCIG gRNA pools.
A. Number of unique sgRNAs detected in each of the MUCIG pools, with the corresponding percentage of library representation annotated.
B. Boxplot of the sgRNA normalized read counts and distribution for each of the MUCIG pools. Box plots display the 25th, 50th, and 75th percentiles of the data, while the whiskers represent the maximum and minimum values within the range, excluding outliers.

Figure S5

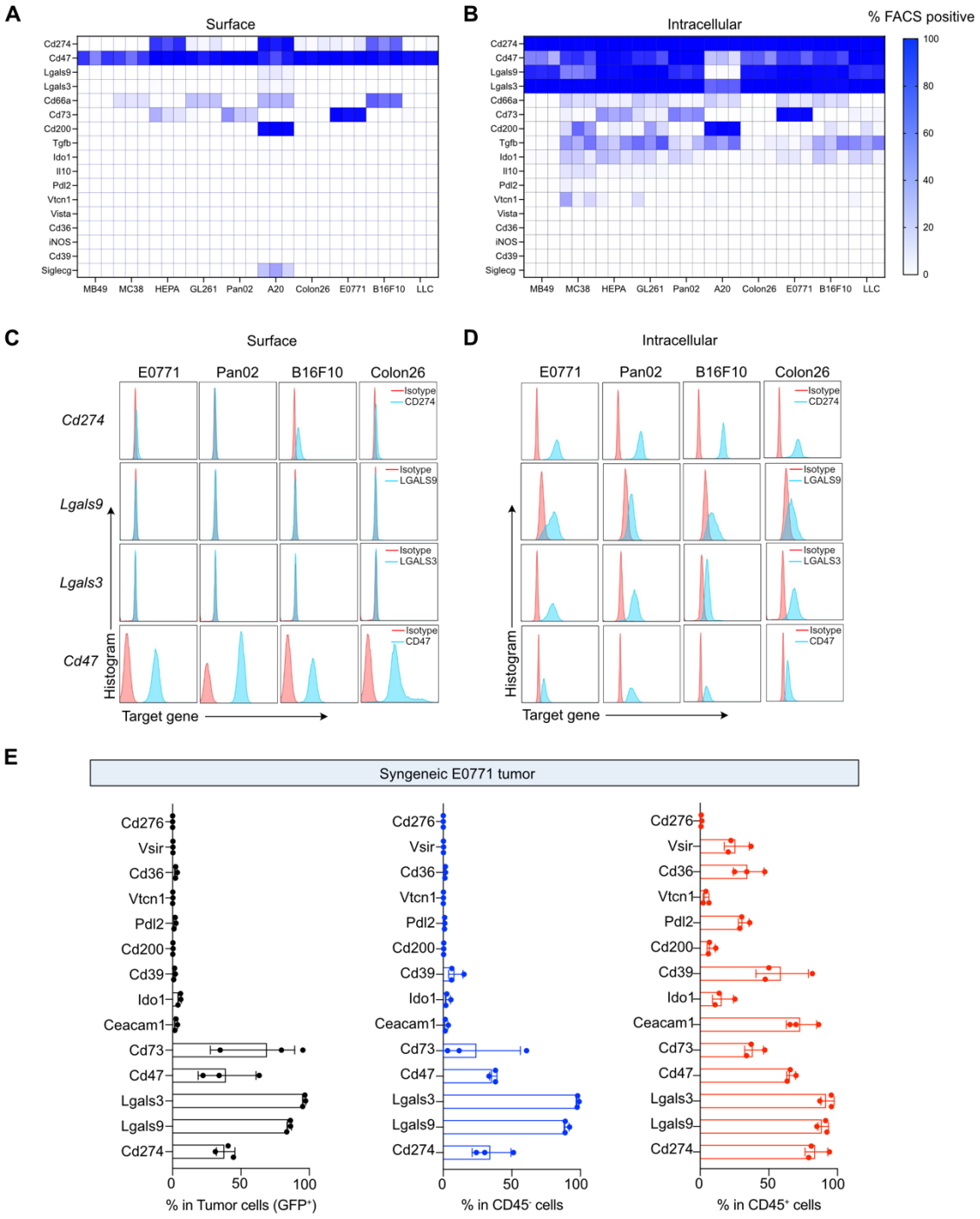

Figure S5. Flow cytometry analysis of immunosuppressive gene expression in cancer cell lines or in the TME.

A-B. Protein-level characterization of a list of immunosuppressive factors across a panel of syngeneic cancer cell lines. Heat maps detailing surface (**A**) and intracellular (**B**) expression of all assayed immunosuppressive factors determined by flow cytometry. Data are expressed in terms of the percentage of total cells that express each marker. (n=3 for each gene per cell line)

C-D. Flow cytometry analysis of PGGC pool targets (*Pdl1/Cd274, Galectin9/Lgals9, Galectin3/Lgals3*, and *Cd47*) in different murine cancer cell lines, either by surface or intracellular staining.
E. Flow cytometry analysis of PGGC pool targets *in vivo* from syngeneic E0771 tumors. C57BL/6 mice were orthotopically injected with $2\times10^{\wedge6}$ E0771-GFP cells. The tumors were harvested at 23 days post injection. Tumor tissues were dissociated for flow cytometry analysis of the indicated markers in each compartment. Each gene was tested in 3 mice (n=3). Data points in this figure are presented as mean ± s.e.m. Details could be found in **Source Data and statistics** excel file.

Figure S6

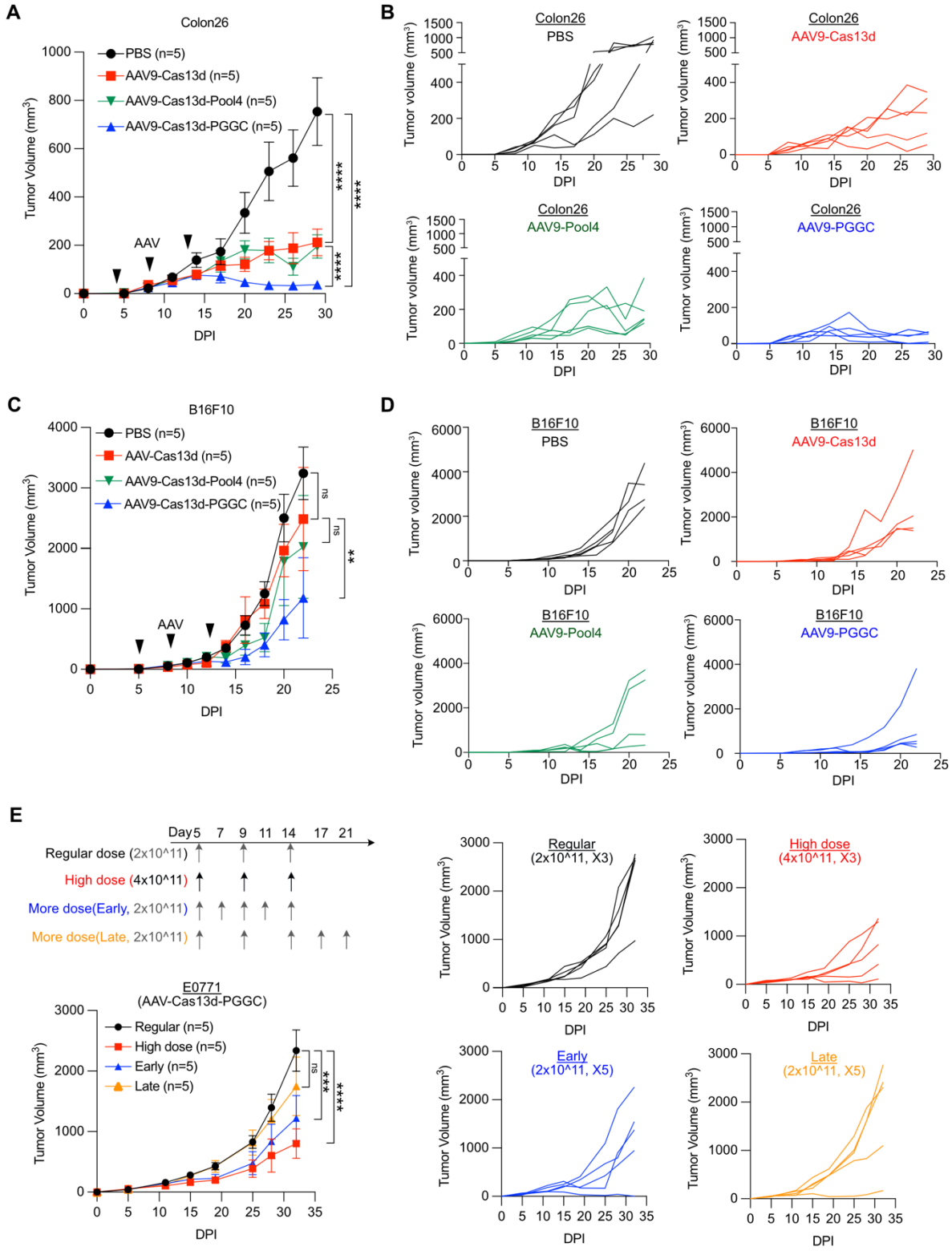

Figure S6: AAV-PGGC therapy demonstrates broad anti-tumor activity in syngeneic models of different cancer types

A. Growth curves of Colon26 tumors intratumorally injected with PBS (n = 5), AAV-Cas13d-Vector (n = 5), AAV- Pool4 (n = 5), and AAV-PGGC (n = 5) ($2\times10^{\wedge11}$) at the timepoints indicated by black arrowheads. This is the same cohort as depicted in Figure 2B.
B. Spider plots of growth curves in (**A**), separated for visibility.
C. Growth curves of B16F10 tumors intratumorally treated with PBS (n = 5), AAV-Cas13d-Vector (n = 5), AAV- Pool4 (n = 5), and AAV-PGGC (n = 5) ($2\times10^{\wedge11}$ AAV per dose) at the timepoints indicated by black arrowheads. This is the same cohort as depicted in Figure 2C.
D. Spider plots of growth curves in (**C**), separated for visibility.
E. Growth curves of E0771 tumors intratumorally injected with AAV-PGGC at indicated dosage and additional injections at the timepoints indicated by black arrowheads.
Data points in this figure are presented as mean ± s.e.m. Statistical significance was assessed by two-way ANOVA. ** $p < 0.01$, *** $p < 0.001$, **** $p < 0.0001$. Non-significant comparisons not shown. Details of statistics in **Source Data and statistics** excel file.

Figure S7

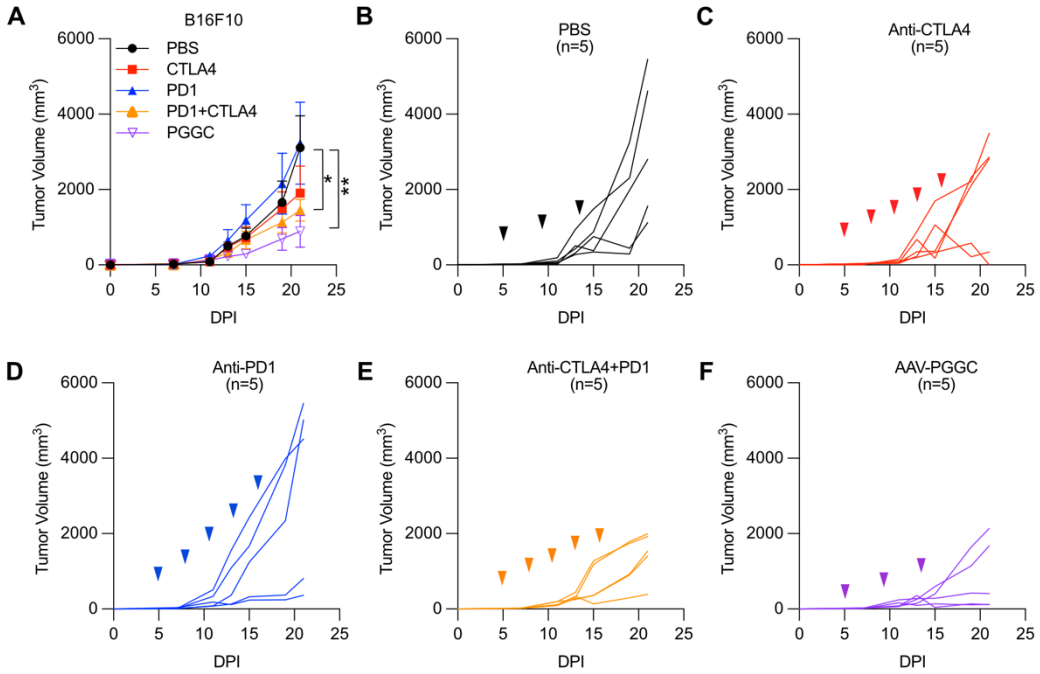

Figure S7: Comparison of AAV-Cas13d-PGGC therapy with immune checkpoint blockade (ICB) therapy in B16F10 melanoma tumor model.

A. $1\times10^{\wedge6}$ B16F10 melanoma cells were subcutaneously injected into C57BL/6 mice. Subsequent treatments included intraperitoneal injections of either anti-PD1 or anti-CTLA4 antibody monotherapy, a combination of anti-PD1 and anti-CTLA4 antibodies, or intratumoral injection of AAV-Cas13d-PGGC at the indicated time points. Tumor growth curves were compared among groups treated with PBS (n=5), anti-CTLA4 (n=5), anti-PD1 (n=5), the combination of anti-CTLA4 and anti-PD1 (n=5), and AAV-Cas13d-PGGC (n=5). Doses were 100μg per antibody injection and $2\times10^{\wedge11}$ vector genomes per AAV injection.

B-F. Spider plots from the tumor growth data in (**A**).

Data points in this figure are presented as mean ± s.e.m. Statistical significance was assessed by two-way ANOVA. * $p < 0.05$, ** $p < 0.01$. Non-significant comparisons are not shown. Details of statistics in **Source Data and statistics** excel file.

Figure S8

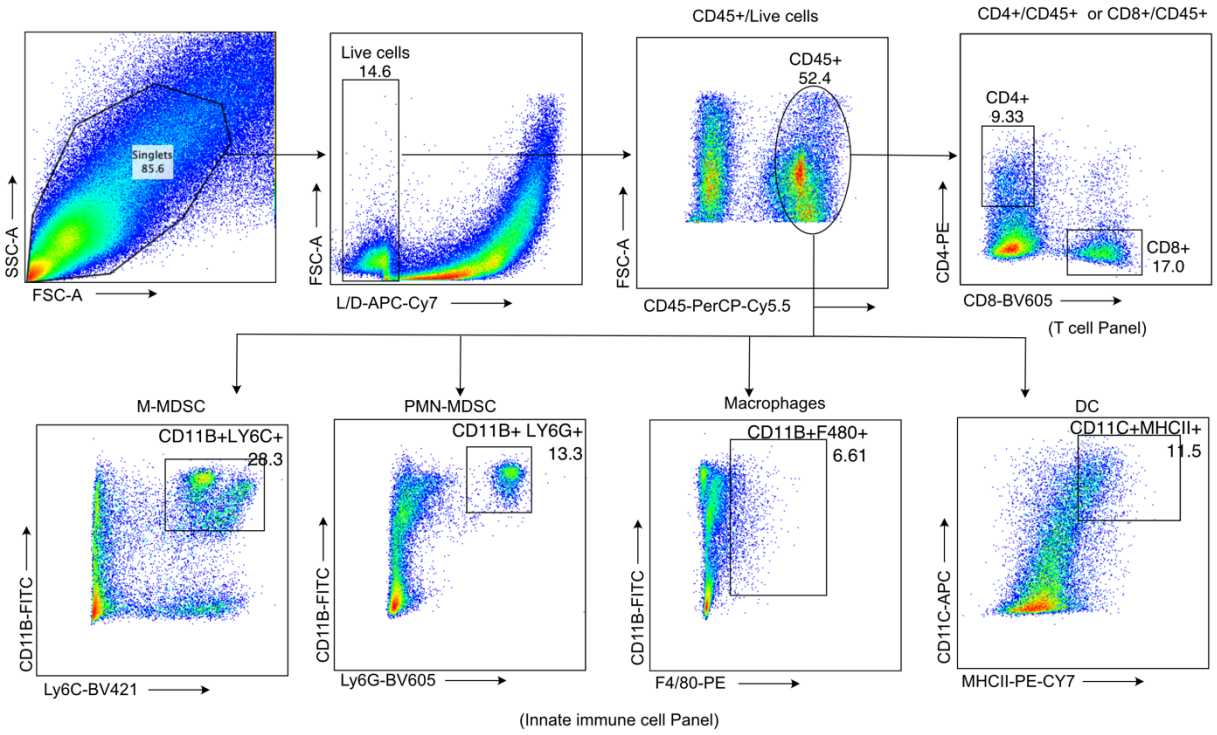

Figure S8. Gating strategy for the tumor infiltrating immune population analysis
The gating strategy for myeloid and lymphocyte cells flow cytometry staining panels are shown. Arrows indicate the parent population that the subsequent plot is gated on. $CD8^+$ T = $CD8^+CD45^+$, $CD4^+$ = $CD4^+CD45^+$, Macrophage = $CD11b^+F4/80^+$, Dendric cell (DC) = $CD11c^+MHCII^+$, MDSC = $CD11b^+Ly6G^+$(PMN-MDSC) + $CD11b^+Ly6C^+$(M-MDSC).

Figure S9

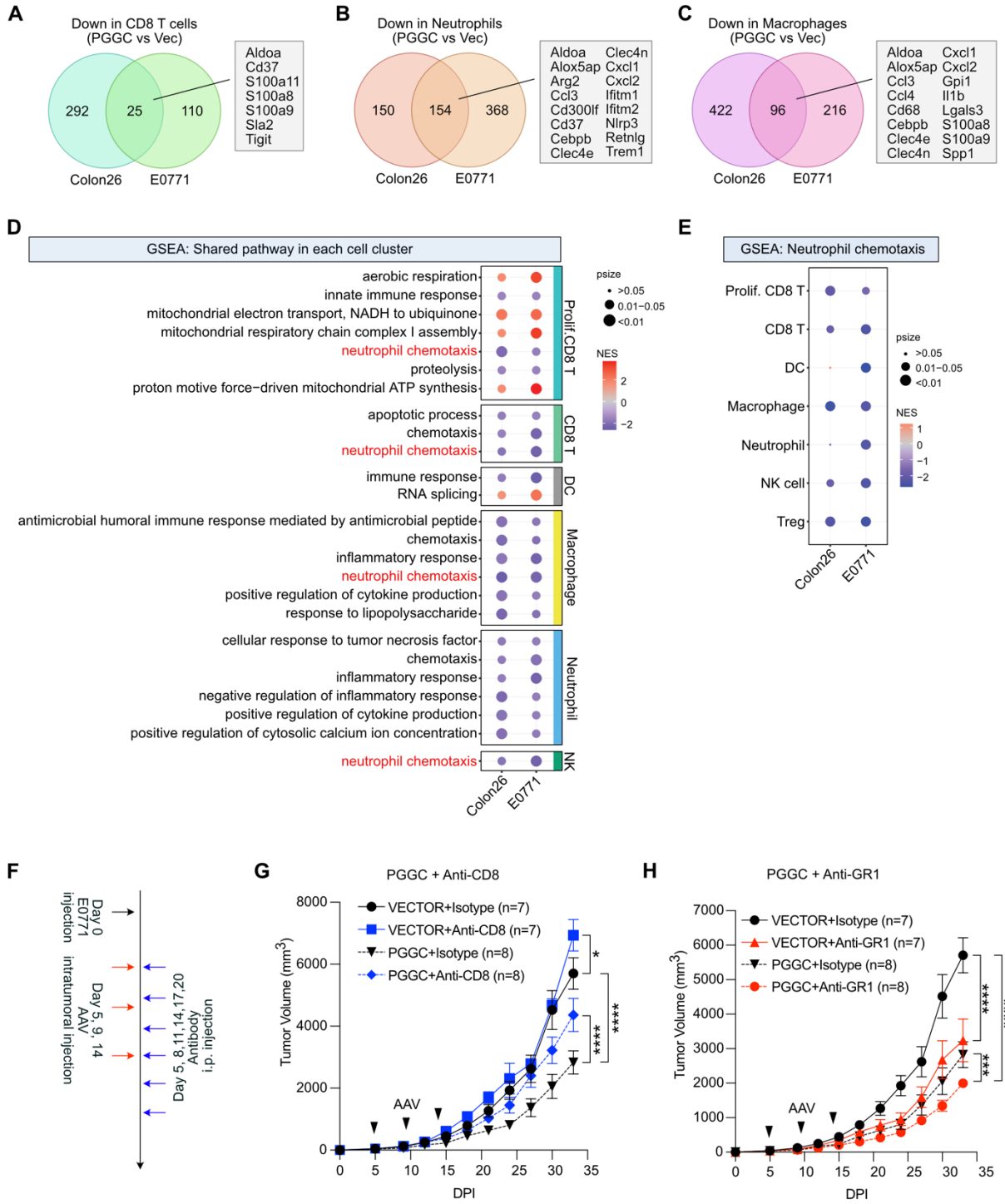

Figure S9. AAV-Cas13d-PGGC treatment remodels the immunosuppressive tumor microenvironment by increasing CD8+ T cells and decreasing neutrophils

A-C. Common signatures of downregulated genes in immune cell populations upon AAV-Cas13d-PGGC treatment, derived from single cell data**.** Overlap of the down-regulated genes in $CD8^{+}$ T

cells (**A**), neutrophils (**B**) and macrophages (**C**), comparing AAV-Cas13d-PGGC vs AAV-Cas13d-Vector in both the Colon26 and E0771 tumor models.
D. Identification of shared gene set enrichment analysis (GSEA) pathway between the E0771 and Colon26 tumor models for each cell cluster.
E. Downregulation of neutrophil chemotaxis pathway in most of the cell types within both E0771 and Colon26 tumor model.
F. Timeline of the experimental design. C57BL/6 mice were orthotopically injected with $2\times10^{\wedge6}$ E0771 cells. Subsequent treatments included intratumoral AAV injections and intraperitoneal (i.p.) antibody injections at indicated time points. Doses were 100 μg per antibody injection and $2\times10^{\wedge11}$ vector genomes per AAV injection.
G-H. Growth curves of AAV-Cas13d-PGGC plus antibody combination treatment in syngeneic orthotopic model (E0771 in C57BL/6 mice). (**G**) PGGC plus anti-CD8 against E0771 breast tumors in C57BL/6, (**H**) PGGC plus anti-GR1 against E0771 breast tumors in C57BL/6. Statistical significance was assessed by two-way ANOVA. * $p < 0.05$, *** $p < 0.001$, **** $p < 0.0001$. Non-significant comparisons are not shown. Details of statistics in **Source Data and statistics** excel file.

Figure S10

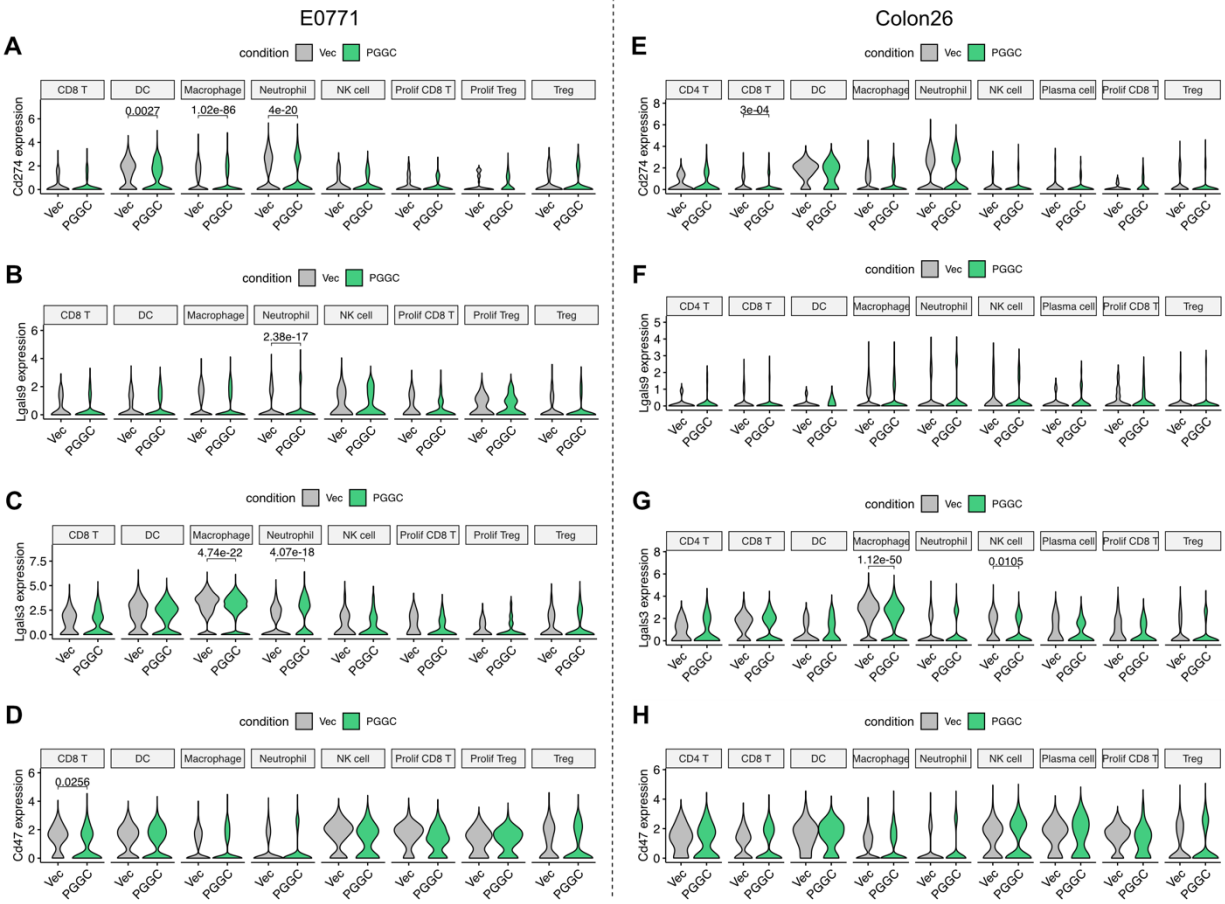

Figure S10: PGGC targeted gene knockdown from the scRNA data

The *in-vivo* targeting gene knockdown in the immune cell population after AAV treatment at day 29 at the RNA level, as analyzed from the single-cell RNA seq data. Statistical significance was assessed by two-tailed unpaired Wilcox test.

A-D. In the E0771 tumor model, the *Cd274/Pdl1* (**A**), *Lgals9*/*Galectin9* (**B**), *Lgals3*/*Galectin3* (**C**) and *Cd47* (**D**) gene knockdown across each cell type.

E-H. In the Colon26 tumor model, *Cd274/Pdl1* (**E**), *Lgals9*/*Galectin9* (**F**), *Lgals3*/*Galectin3* (**G**) and *Cd47* (**H**).

Figure S11

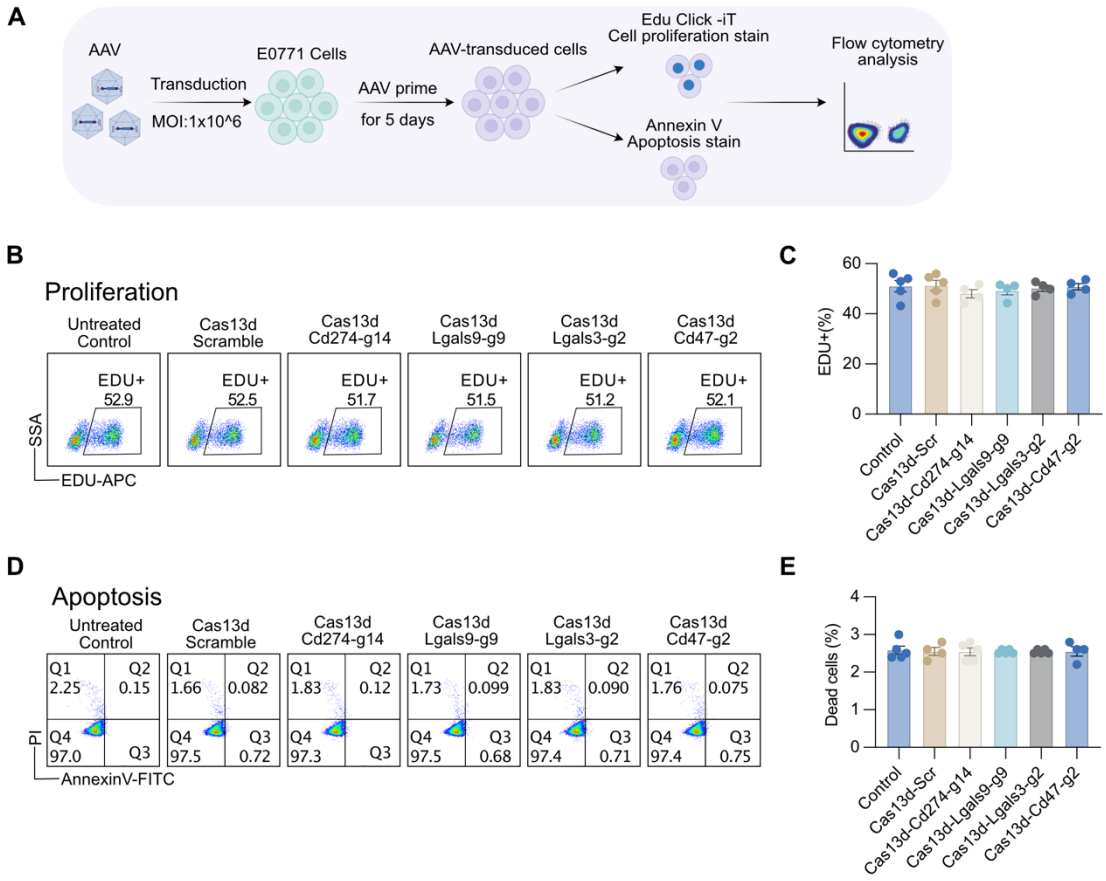

Figure S11: PGGC knockdown by CRISPR-Cas13d has no cell-intrinsic effect on tumor cell growth and death

A. Schematic of cell proliferation and cell death assay following PGGC (*Cd274, Lgals9, Lgals3, Cd47*) gene knockdown by AAV-Cas13d in tumor cells. E0771 tumor cells were transduced with AAV-Cas13d and the presence of PGGC-targeting gRNAs for 5 days, and then tumor cell proliferation was tested by EdU assay, and cell death was tested by annexin V and propidium iodide (PI) staining.

B-C. Flow cytometry analysis and statistical quantification showed that PGGC (*Cd274, Lgals9, Lgals3, Cd47*) knockdown does not affect tumor growth. (n>=4, each group)

D-E. Tumor cell apoptosis was detected by annexin V and PI staining, with quantification of Q1+Q2+Q3. (n>=4, each group)

Data points in this figure are presented as mean ± s.e.m. Statistical significance was assessed by one-way ANOVA test. Non-significant comparisons are not shown. Details of statistics in **Source Data and statistics** excel file.

Figure S12

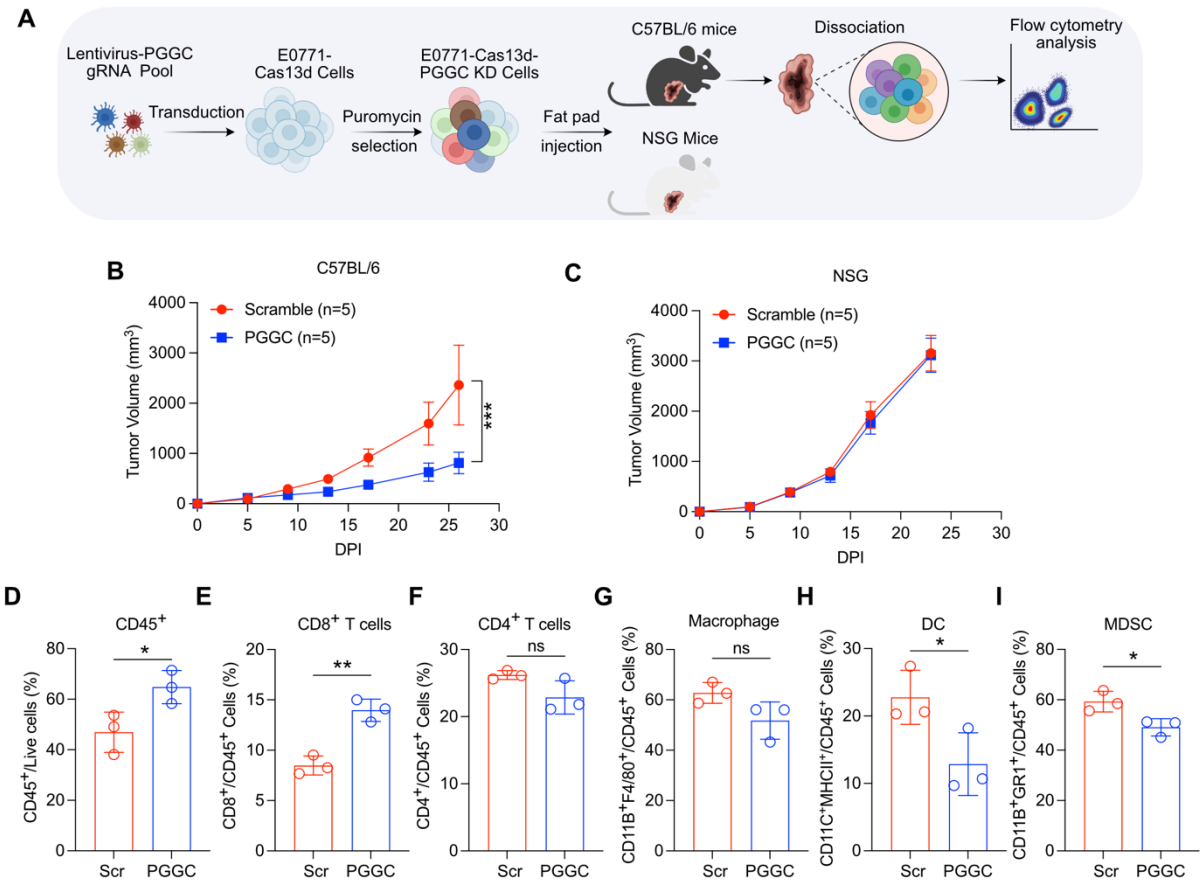

Figure S12: The anti-tumor effect of Cas13d-PGGC is mediated by the immune system.
A. Schematic of the experiment design: PGGC genes were knockdown in E0771-Cas13d cells using a lentivirus mini-pool. Then, $1\times10^{\wedge7}$ tumor cells with 50% Matrigel were orthotopically injected into the fat pads of either immunocompetent (C57BL/6) or immunodeficient (NSG) mice. Tumor volume was measured every 3 to 5 days.
B. In immunocompetent mice, PGGC gene knockdown led to reduced tumor burden when comparing to the scramble control group (n=5, each group).
C. In immunodeficient (NSG) mice, there is no significant difference in tumor growth between PGGC knockdown and scramble control group, (n=5, each group).
D-I. Quantification of immune cells in the E0771 tumor microenvironment via flow cytometry analysis. Tumors from the immunocompetent mice were dissociated, and the infiltrated immune cells were analyzed by flow cytometry on day14 after injection (n=3 for each group). (**D**) the percentage of $CD45^+$ immune cells relative to total live cells; (**E**) Percentage of total $CD8^+$ T cells; (**F**) Percentage of total $CD4^+$ T cells; (**G**) Percentage of macrophages ($CD11B^+F4/80^+$); (**H**) dendritic cells ($CD11C^+MHCII^+$); (**I**) MDSC among tumor infiltrating $CD45^+$ immune cells.
Data points in this figure are presented as mean ± s.e.m. Statistical significance was assessed by two-way ANOVA (**B, C**), and two-sided unpaired *t* test (**D-I**). * $p < 0.05$, ** $p < 0.01$, *** $p < 0.001$. Details of statistics in **Source Data and statistics** excel file.

Figure S13

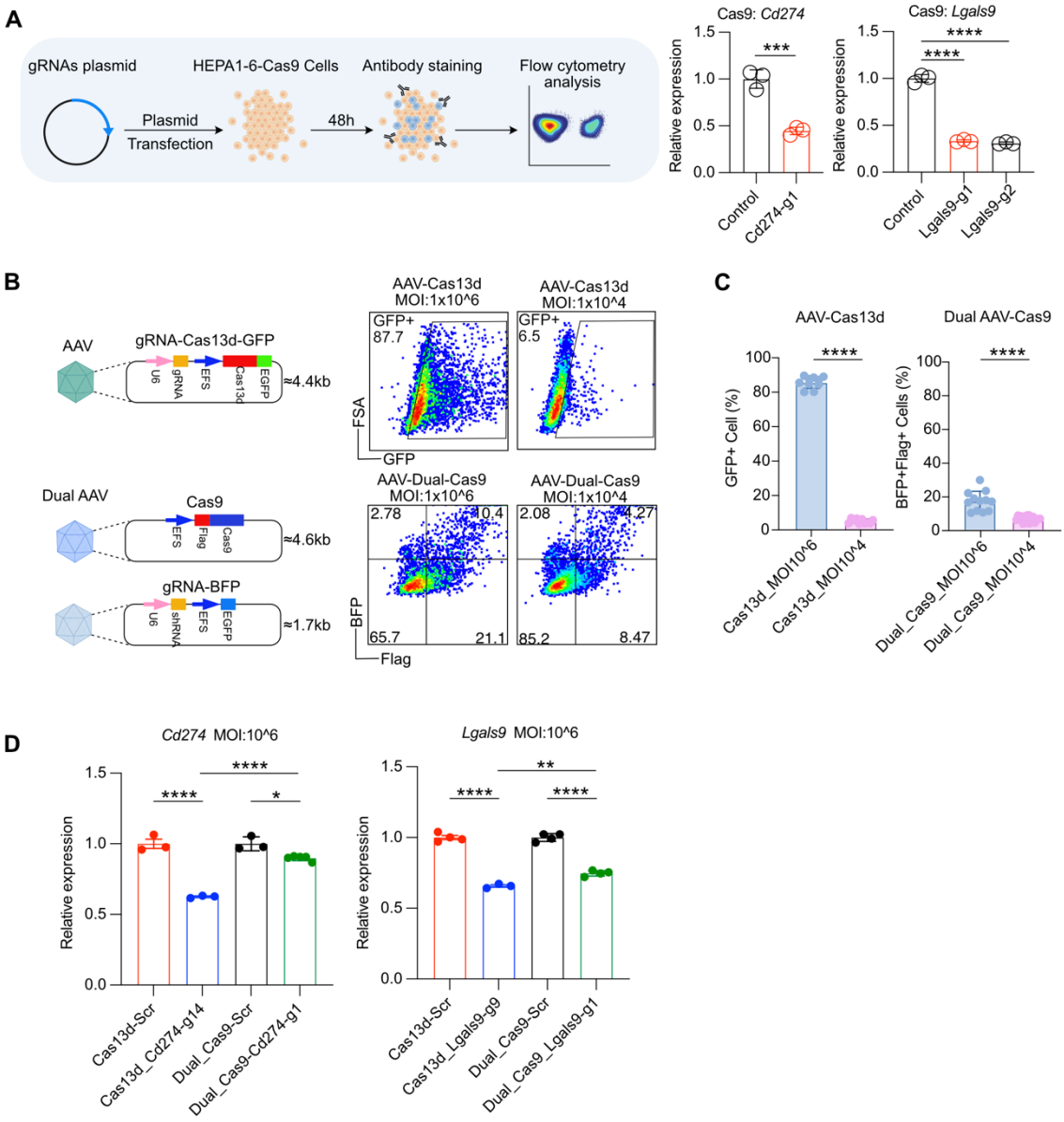

Figure S13: Comparison of the gene repression efficacy of Cas13d and Cas9.

A. Evaluation of Cas9-mediated gene repression in Hepa-1-6 cells. gRNA plasmids were transfected into Hepa-Cas9 expressing cells, and 2 days later CD274 and LGALS9 expression at the protein level was analyzed by flow cytometry. (n=3, each group)

B. Flow cytometry representation of cells transduced by AAV-Cas13d, indicated by GFP^+, or cells transduced by dual AAV system of (Cas9 and gRNA), indicated by $Flag^+$ and BFP^+ double positive cells. Flow cytometry was performed 5 days post AAV infection.

C. Quantification of the transduction efficiencies from panel B. Evaluation of the Cas13d and dual Cas9 transduction efficiency by AAV delivery in vitro at MOIs of $1\times10^{\wedge6}$ and $1\times10^{\wedge4}$. (n>=10, each group)

D. Knockdown efficiency of AAV-Cas13d or dual AAV-Cas9 when targeting *Cd274* and *Lgals9*. (n>=3, each group)

Data points in this figure are presented as mean ± s.e.m. Statistical significance was assessed by two-sided unpaired *t* test (**A, C**), and one-way ANOVA (**D**). * $p < 0.05$, ** $p < 0.01$, *** $p < 0.001$, **** $p < 0.0001$. Non-significant comparisons not shown. Details of statistics in **Source Data and statistics** excel file.

Figure S14

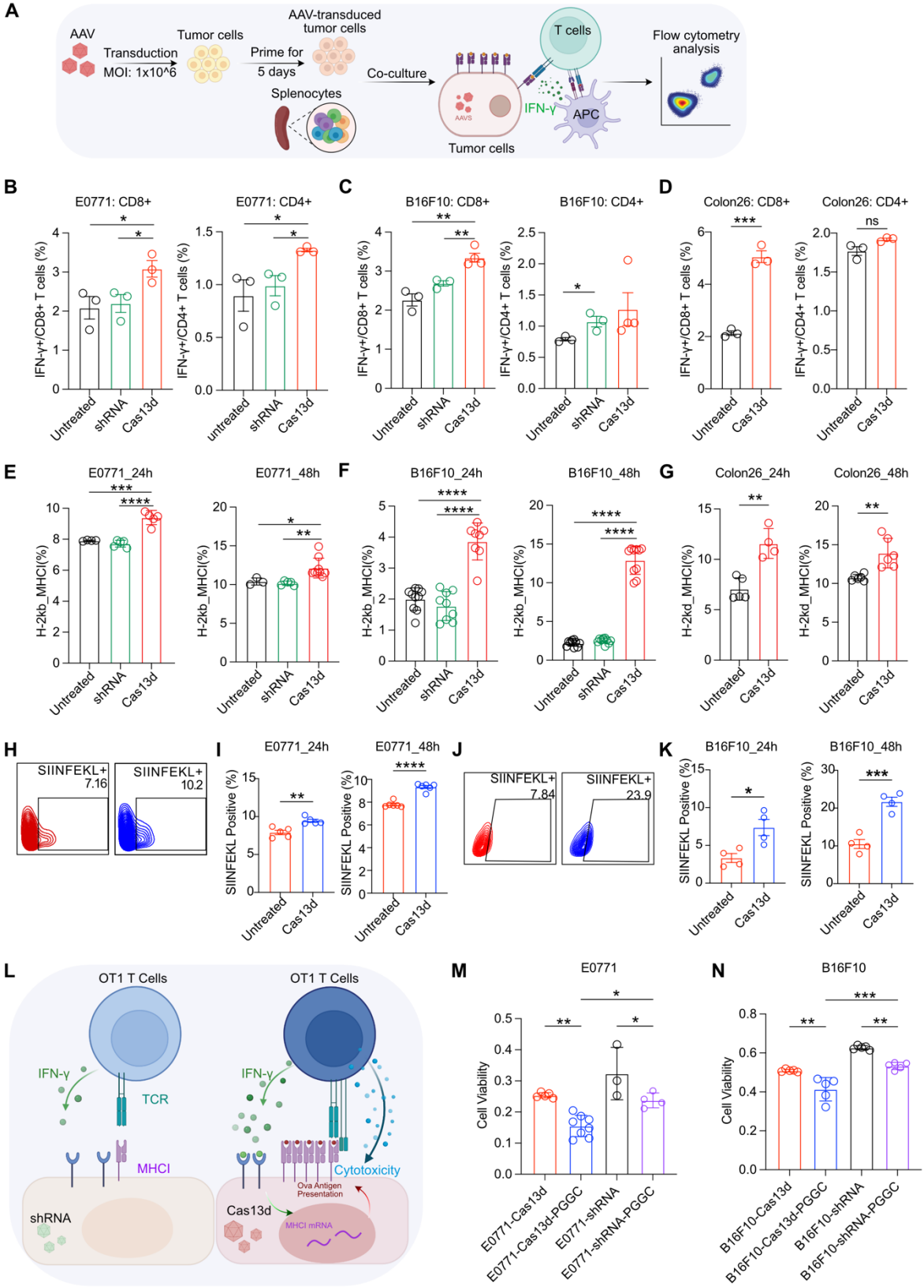
A
AAV
Transduction
MOI: 1x10^6
Tumor cells
Prime for
5 days
AAV-transduced
tumor cells
Splenocytes
Co-culture
T cells
IFN-γ
APC
Tumor cells
Flow cytometry
analysis
B
E0771: CD8+
E0771: CD4+
C
B16F10: CD8+
B16F10: CD4+
D
Colon26: CD8+
Colon26: CD4+
IFN-γ+/CD8+ T cells (%)
IFN-γ+/CD4+ T cells (%)
Untreated
shRNA
Cas13d
E
E0771_24h
E0771_48h
F
B16F10_24h
B16F10_48h
G
Colon26_24h
Colon26_48h
H-2kb_MHCI(%)
H-2kd_MHCI(%)
H
SIINFEKL+
7.16
SIINFEKL+
10.2
I
E0771_24h
E0771_48h
J
SIINFEKL+
7.84
SIINFEKL+
23.9
K
B16F10_24h
B16F10_48h
SIINFEKL Positive (%)
L
OT1 T Cells
OT1 T Cells
IFN-γ
TCR
MHCI
shRNA
IFN-γ
Cytotoxicity
Ova Antigen
Presentation
Cas13d
MHCI mRNA
M
E0771
N
B16F10
Cell Viability
E0771-Cas13d
E0771-Cas13d-PGGC
E0771-shRNA
E0771-shRNA-PGGC
B16F10-Cas13d
B16F10-Cas13d-PGGC
B16F10-shRNA
B16F10-shRNA-PGGC

Figure S14: AAV-Cas13d promotes anti-tumor immunity by stimulating IFN-γ production and enhancing antigen presentation

A. Experimental design schematic for assessing the immunogenicity of AAV-Cas13d *in-vitro*. Tumor cells were treated with either AAV-Cas13d or AAV-shRNA non-targeting vectors for five days, followed by co-culture with splenocytes (including T cells and antigen presenting cells (APCs)) for 24 hours. IFN-γ expression in T cells was then assessed by flow cytometry.

B-D. Quantification of intracellular IFN-γ expression in $CD4^+$ and $CD8^+$ T cells 24 hours after co-culture with E0771 (**B**), B16F10 (**C**) and Colon26 cells (**D**) treated with AAV-shRNA or AAV-Cas13d. Splenocytes from C57BL/6 mice were used for E0771 and B16F10 co-culture assays, while splenocytes from BALB/c mice were used for Colon26 cells. (n>=3, each group)

E-G. Expression level of MHC-I on E0771 (**E**), B16F10 (**F**) and Colon26 (**G**) cells after 24 hours (left) or 48 hours (right) co-culture with splenocytes. H-2kb was tested for E0771 and B16F10 cells, and H-2kd was tested for Colon26 cells. (n>=3, each group)

H-K. Presentation of SIINFEKL peptides by MHC-I on E0771-Ova cells (**H, I**) and B16F10-Ova cells (**J, K**), after co-culture with splenocytes for 24h or 48h. (n>=3, each group)

L. Schematic depicting the mechanism by which AAV-Cas13d promotes T cell cytotoxicity.

M-N. Comparison of tumor cell viability among Ova-expressing E0771 (**M**) and B16F10 (**N**) tumor cells infected with AAV-Cas13d, AAV-Cas13d-PGGC, AAV-shRNA, or AAV-shRNA-PGGC for five days, followed by co-culture with cognate OT-I T cells. (n>=3, each group)

Data points in this figure are presented as mean ± s.e.m. Statistical significance was assessed by two-sided unpaired *t* test (**B-K**) and one-way ANOVA (**M, N**). $^{**}p < 0.05$, $^{**}\ p < 0.01$, $^{***}\ p < 0.001$, $^{****}\ p < 0.0001$. Non-significant comparisons not shown. Details of statistics in **Source Data and statistics** excel file.

Figure S15

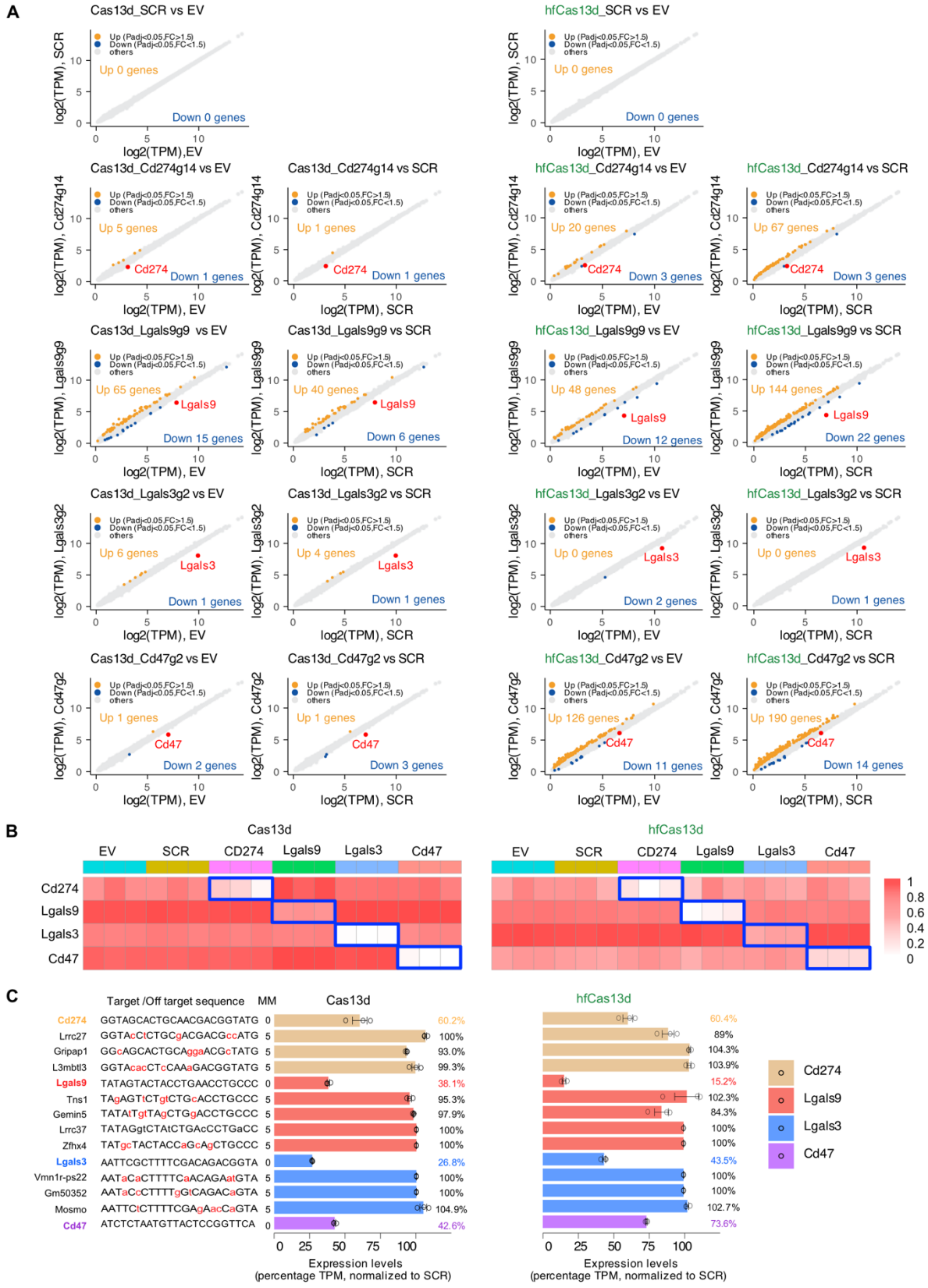
A
Cas13d_SCR vs EV
Up 0 genes
Down 0 genes
hfCas13d_SCR vs EV
Up 0 genes
Down 0 genes
Cas13d_Cd274g14 vs EV
Up 5 genes
Down 1 genes
Cas13d_Cd274g14 vs SCR
Up 1 genes
Down 1 genes
hfCas13d_Cd274g14 vs EV
Up 20 genes
Down 3 genes
hfCas13d_Cd274g14 vs SCR
Up 67 genes
Down 3 genes
Cas13d_Lgals9g9 vs EV
Up 65 genes
Down 15 genes
Cas13d_Lgals9g9 vs SCR
Up 40 genes
Down 6 genes
hfCas13d_Lgals9g9 vs EV
Up 48 genes
Down 12 genes
hfCas13d_Lgals9g9 vs SCR
Up 144 genes
Down 22 genes
Cas13d_Lgals3g2 vs EV
Up 6 genes
Down 1 genes
Cas13d_Lgals3g2 vs SCR
Up 4 genes
Down 1 genes
hfCas13d_Lgals3g2 vs EV
Up 0 genes
Down 2 genes
hfCas13d_Lgals3g2 vs SCR
Up 0 genes
Down 1 genes
Cas13d_Cd47g2 vs EV
Up 1 genes
Down 2 genes
Cas13d_Cd47g2 vs SCR
Up 1 genes
Down 3 genes
hfCas13d_Cd47g2 vs EV
Up 126 genes
Down 11 genes
hfCas13d_Cd47g2 vs SCR
Up 190 genes
Down 14 genes
B
Cas13d
hfCas13d
EV
SCR
CD274
Lgals9
Lgals3
Cd47
C
Target /Off target sequence
MM
Cas13d
hfCas13d
Expression levels
(percentage TPM, normalized to SCR)

Figure S15: Transcriptome-wide off target and collateral activity analysis for Cas13d and hf Cas13d

A. Scatter plots showing the transcriptome-wide gene expression and collateral activity analysis for both Cas13d and hf Cas13d, comparing target guide RNAs with controls, including EV (Empty Vector), and SCR (Scramble guide RNA). Benjamini-Hochberg adjusted p-values (Padj) were calculated using an outlier test compared to studentized residuals from linear regression analysis.

B. Heatmap showing the on-target knockdown efficiency of the targeting genes across all the group settings. TPM values from the 36 sample from both Cas13d and hfCas13d cohorts were normalized row wised by resealing to a range of 0 to 1.

C. Off-target sites with one or more mismatches were analyzed, and their relative expression levels were compared to the SCR control. Data points in this figure are presented as mean ± s.e.m. (n=3, each group)

Figure S16

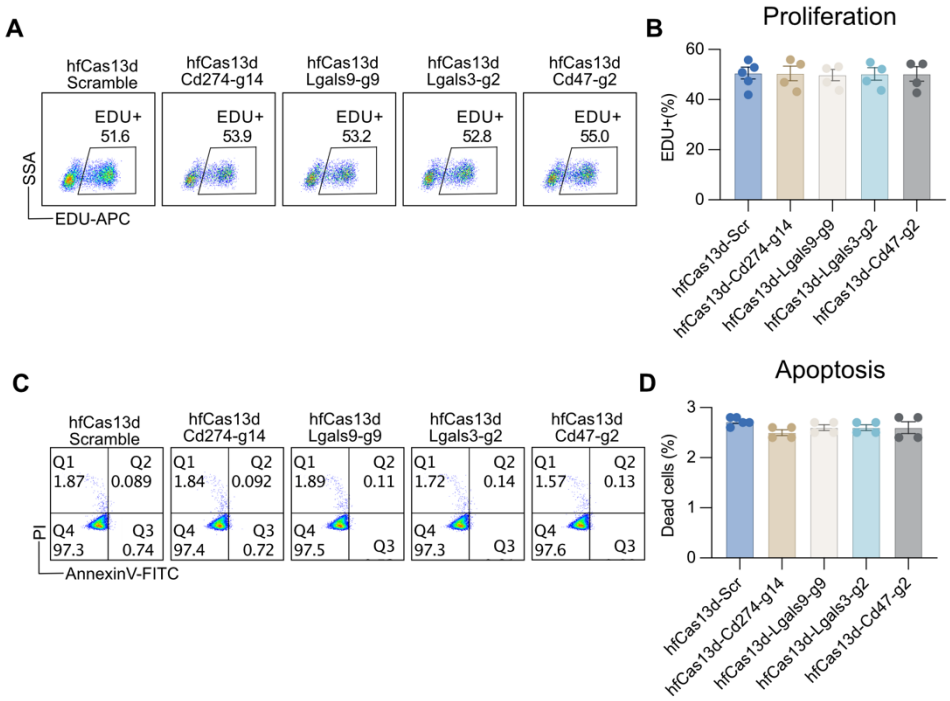

Figure S16: CRISPR-hfCas13d does not exhibit cell-intrinsic effects on tumor cell growth or death

A-B. Flow cytometry analysis and quantification showing that AAV-hfCas13d-PGGC single gene knockdown does not affect tumor growth. E0771 tumor cells were transduced with AAV-hfCas13d for 5 days, and then tumor cell proliferation was tested by EdU assay. (n>=4, each group)

C-D. Tumor cell apoptosis was detected by annexin V and PI staining, with quantification of Q1+Q2+Q3. (n>=4, each group)

Data points in this figure are presented as mean ± s.e.m. Statistical significance was assessed by one-way ANOVA test. Non-significant comparisons are not shown. Details of statistics in **Source Data and statistics** excel file.

Source data and statistics

Source data and statistics of non-NGS type data are provided in an excel file.

Supplemental Datasets

Supplemental datasets include processed data for single cell RNA-seq PGGC knockdown analysis (related to Figure S10), transcriptome-wide collateral activity analysis (related to Figure S15).

Supplemental Tables

Supplemental Tables include commercial reagents used in this study, DNA oligonucleotide sequences (non-library)